Title

Hepatic Fibrosis: Evaluation with Semiquantitative Contrast-enhanced CT

Journal

Radiology, 266(1)

ISSN

0033-8419

Authors

Varenika, Vanja

Fu, Yanjun

Maher, Jacquelyn J

et al.

Publication Date

2013

DOI

10.1148/radiol.12112452

Peer reviewed

Hepatic Fibrosis: Evaluation with Semiquantitative Contrast-enhanced CT[1]

Vanja Varenika, MD
Yanjun Fu, PhD
Jacquelyn J. Maher, MD
Dongwei Gao, MD
Sanjay Kakar, MD
Miguel C. Cabarrus, MD
Benjamin M. Yeh, MD

Purpose: To evaluate the feasibility of using contrast material–enhanced computed tomographic (CT) measurements of hepatic fractional extracellular space (fECS) and macromolecular contrast material (MMCM) uptake to measure severity of liver fibrosis.

Materials and Methods: All procedures were approved by and executed in accordance with University of California, San Francisco, institutional animal care and use committee regulations. Twenty-one rats that received intragastric CCl_4 for 0–12 weeks were imaged with respiratory-gated micro-CT by using both a conventional contrast material and a novel iodinated MMCM. Histopathologic hepatic fibrosis was graded qualitatively by using the Ishak fibrosis score and quantitatively by using morphometry of the fibrosis area. Hepatic fECS and MMCM uptake were calculated for each examination and correlated with histopathologic findings by using uni- and multivariate linear regressions.

Results: Ishak fibrosis scores ranged from a baseline of 0 in untreated animals to a maximum of 5. Histopathologic liver fibrosis area increased from 0.46% to 3.5% over the same interval. Strong correlations were seen between conventional contrast-enhanced CT measurements of fECS and both the Ishak fibrosis scores (R^2 = 0.751, $P < .001$) and the fibrosis area (R^2 = 0.801, $P < .001$). Strong negative correlations were observed between uptake of MMCM in the liver and Ishak fibrosis scores (R^2 = 0.827, $P < .001$), as well as between uptake of MMCM in the liver and fibrosis area (R^2 = 0.643, P = .001). Multivariate linear regression analysis showed a trend toward independence for fECS and MMCM uptake in the prediction of Ishak fibrosis scores, with an R^2 value of 0.86 (P = .081 and P = .033, respectively).

Conclusion: Contrast-enhanced CT measurements of fECS and MMCM uptake are individually capable of being used to estimate the degree of early hepatic fibrosis in a rat model.

Supplemental material: *http://radiology.rsna.org/lookup/suppl/doi:10.1148/radiol.12112452/-/DC1*

[1] From the Department of Radiology and Biomedical Imaging, University of California, San Francisco, 505 Parnassus Ave, Box 0628, M-372, San Francisco, CA 94143-0628. Received December 16, 2011; revision requested January 23, 2012; revision received July 5; final version accepted August 1. Supported by a Pilot Award from the UCSF Liver Center (P30 DK026743) and the Howard Hughes Medical Institute (V.V., M.C.C.). **Address correspondence to** B.M.Y. (e-mail: *ben.yeh@ucsf.edu*).

There is a pressing need for an accurate and noninvasive method with which to reliably stage hepatic fibrosis. Liver biopsy is the most widely accepted reference standard in the assessment of hepatic fibrosis, but it is prone to interobserver variation (1,2) and sampling error (3–5), and it is associated with pain in 40% of cases and with major complications in 0.5% (6). Current serum biomarker panels and noninvasive imaging methods are well suited for use in the identification of advanced liver fibrosis, but they are unreliable in distinguishing between early and intermediate stages of disease (7–12) where therapy is most likely to be effective (13–19). The increasing availability of treatments that halt or even reverse hepatic fibrosis (20,21) calls for improvements in noninvasive measures of fibrosis to permit accurate monitoring of responses to therapy (20–22). Development of a noninvasive imaging technique would also enable wider screening and closer monitoring of patients at risk for developing diffuse liver disease.

The liver is generally considered to be composed of three distinct spaces: the fractional intravascular space, fractional intracellular space, and fractional extravascular extracellular space (fEES) (22). The essential histopathologic feature of hepatic fibrosis is the expansion of the fEES secondary to the deposition of collagen and matrix proteins (Fig 1) (23). The fEES accounts for approximately 15% of the total fluid space in normal livers, but it can gradually expand to account for more than 50% of the volume in patients with advanced disease (24). No prior study has evaluated the potential of using noninvasive imaging to quantify the expansion of the fEES as a means of staging hepatic fibrosis. Progressive hepatic fibrosis is also closely associated with a decrease in the free passage of macromolecules from the fractional intravascular space to the fEES due to decreased permeability of the sinusoidal endothelial cells (25,26). Decreased free transit of nutrients and macromolecules, such as albumin, between the fractional intravascular space and the fEES correlate well with chronic liver disease severity (27). Unfortunately, published procedures to test macromolecule uptake by the liver are highly invasive (27) or technically involved (26).

While measurement of the fEES is challenging, quantification of the fractional extracellular space (fECS), which is the sum of the fEES and fractional intravascular space, is relatively simple at computed tomographic (CT) scanning. All current water-soluble conventional noncholangiographic CT contrast materials, also termed *low-molecular-weight contrast materials*, pass freely between the intravascular space and the fEES of the liver but are not taken up by living cells (28). The ability of small molecules to pass from the intravascular space to the fEES is high, even in the setting of cirrhosis (27). As such, soon after parenteral injection, the distribution of conventional low-molecular-weight contrast material reaches an equilibrium in which the concentration of contrast material is similar between the intravascular space and the fEES. Images acquired at this time are commonly referred to as equilibrium phase images. Since the concentration of contrast material at CT is directly proportional to the CT attenuation, the fECS is simply estimated as the ratio of enhancement of the liver parenchyma to enhancement of the blood pool multiplied by the difference of 1 minus the hematocrit value during the equilibrium phase. Furthermore, macromolecule uptake across microvessels can be readily measured using macromolecular contrast materials (MMCMs) (29,30). In the present study, we evaluated the potential of using contrast material–enhanced CT measurements of hepatic fECS and MMCM uptake to estimate the degree of hepatic fibrosis in a CCl_4 rat model of chronic liver disease.

Advances in Knowledge

- CT quantification of liver fractional extracellular space (fECS) has a strong correlation with the degree of hepatic fibrosis, as determined with Ishak fibrosis scores ($R^2 = 0.751$) and morphometric measurements of liver fibrosis area ($R^2 = 0.801$).
- CT quantification of liver macromolecular contrast material (MMCM) uptake has a strong negative correlation with the quantity of hepatic fibrosis, as determined with Ishak fibrosis scores ($R^2 = 0.827$) and morphometric measurements of liver fibrosis area ($R^2 = 0.643$).

Implication for Patient Care

- Contrast-enhanced CT measurements of fECS and MMCM uptake may be useful semiquantitative markers of liver fibrosis and could enable noninvasive monitoring of liver disease severity.

Materials and Methods

Animal Model

All procedures were approved by and executed in accordance with the regulations of the University of California, San Francisco, institutional animal care and use committee. Experiments were performed with a cohort of 21 Sprague-Dawley rats (Charles River Laboratories; Wilmington, Mass), each

Published online before print
10.1148/radiol.12112452 **Content code:** GI
Radiology 2013; 266:151–158

Abbreviations:
fECS = fractional extracellular space
fEES = fractional extravascular extracellular space
MMCM = macromolecular contrast material
ROI = region of interest

Author contributions:
Guarantors of integrity of entire study, V.V., B.M.Y.; study concepts/study design or data acquisition or data analysis/interpretation, all authors; manuscript drafting or manuscript revision for important intellectual content, all authors; approval of final version of submitted manuscript, all authors; literature research, V.V., Y.F., B.M.Y.; experimental studies, all authors; statistical analysis, V.V., B.M.Y.; and manuscript editing, all authors

Funding:
This research was supported by the National Institutes of Health (grants R01CA122257 and R21EB013816).

Conflicts of interest are listed at the end of this article.

See also Science to Practice in this issue.

initially weighing 139–150 g. Eighteen rats underwent a 2-week phenobarbital induction to sensitize the livers to CCl_4 by using 35 mg/dL phenobarbital in drinking water (31). Hepatic fibrosis was then induced by administering weekly intragastric CCl_4 doses, as previously described by Proctor and Chatamra (32). Every 2 weeks for a total of 12 weeks after the start of CCl_4 administration, three randomly selected rats underwent CT imaging and then were sacrificed for histopathologic analysis of the liver. Each group was imaged a week after the last dose of CCl_4 was administered. Three control rats were scanned at the beginning of the study without receiving any phenobarbital or CCl_4. The hematocrit level was measured in each rat just prior to conventional contrast-enhanced CT.

Figure 1

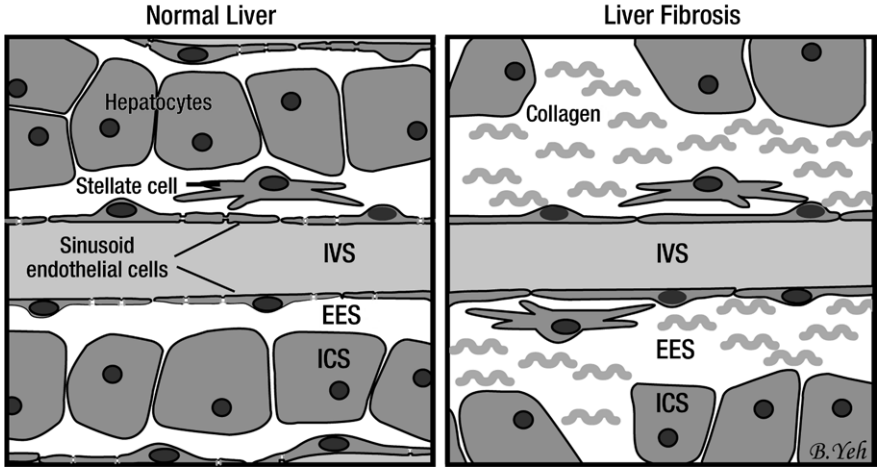

Figure 1: Schematic representation of liver spaces and histology in a normal liver and a liver with fibrosis. The three principle physiologic spaces in normal liver tissue are intravascular space *(IVS)*, intracellular space *(ICS)*, and extravascular extracellular space *(EES)*. The fECS is the sum of the intravascular space and extravascular extracellular space. Fenestrations are present in normal liver sinusoid endothelial cells. In liver fibrosis, the extracellular space enlarges due to collagen deposition in the space of Disse, and sinusoid endothelial cell fenestrations diminish in number or disappear.

Contrast Material

Conventional extracellular contrast material (iohexol, Omnipaque 300; GE Healthcare, Madison, Wis) was used as the low-molecular-weight contrast material. The MMCM used in this study, PEG12000-Gen4-IOB, was synthesized according to a previously reported method (33). This iodine-containing macromolecule has a blood pool distribution with an elimination half-life of 36 minutes and a molecular weight of 36 kDa, and it behaves like a protein of approximately 100 kDa based on size-exclusion high-performance liquid chromatography analysis. This contrast-enhancing macromolecule was formulated as a solution for intravenous injection with a concentration of 75 mg of iodine per milliliter. More information about the synthesis and attributes of this compound can be found in Appendix E1 (online). The dose of both contrast materials used in this study was 600 mg of iodine per kilogram of body weight.

CT Scans

Each animal was imaged on two consecutive days, with low-molecular-weight contrast material administered on the 1st day and MMCM administered on the 2nd day. The CT scans were conducted with a micro-CT scanner (Inveon microCAT II; Siemens Healthcare, Malvern, Pa) with the following parameters: 80-kVp x-ray tube voltage, 500 μA, 175-msec exposure time per step, and 180 angular samples over 360° in a step-and-shoot mode. The data were acquired in a 4096 × 3968 × 180 matrix and were reconstructed by using a modified cone-beam Feldkamp algorithm developed by Exxim Computing (Pleasanton, Calif) resulting in 512 × 512 × 448 matrices with an isotropic pixel size of 95.34 μm. Prospective respiratory gating was performed by using a pressure-sensitive pad (Biovet; M2M Imaging, Cleveland, Ohio) placed on the abdomen of the animals for all CT scans. For each imaging session, both a precontrast series and a postcontrast series were acquired, with an average scanning time of 9 minutes per series, which was started approximately 1 minute after contrast material injection. As such, the contrast material was in the equilibrium phase of enhancement for the majority of the imaging time.

Image Analysis

All images were analyzed in consensus by a trainee (V.V.) and an attending abdominal radiologist with 10 years of subspecialty experience (B.M.Y.) using a Digital Imaging and Communications in Medicine image viewer (OsiriX version 3.8.1; Pixmeo, Geneva, Switzerland). This analysis was performed sequentially over time, and observers were blinded to the results of histopathology and morphometry but not to CCl_4 exposure. Hepatic attenuation was measured by calculating the average attenuation value (in Hounsfield units) of four 0.250-cm^2 regions of interest (ROIs), with two ROIs placed in each hepatic lobe (Fig 2) with care to avoid large blood vessels or areas of obvious image artifact. The blood pool attenuation was measured by calculating the average attenuation value for three 0.35-mm^2 ROIs placed in the thoracic inferior vena cava (Fig 2), with care to confine the ROI to the lumen of the blood vessel. The hepatic fECS was calculated by using the averaged ROI values from the conventional contrast-enhanced scan and the following equation: $fECS = (L_{post} - L_{pre}) / (A_{post} - A_{pre}) \times (1 - Hct)$, where L_{post} and L_{pre} are post- and precontrast liver ROI values, respectively; A_{post} and A_{pre} are post- and precontrast aorta ROI

values, respectively; and Hct is the hematocrit level. The hepatic MMCM uptake was calculated by using similar averaged ROI values from the MMCM scans and the same equation.

Ishak Fibrosis Score

The degree of hepatic fibrosis was staged pathologically by using picrosirius red-stained liver slices. Two slices, one from each lobe of the liver, were assigned an Ishak fibrosis score (0–6) and an Ishak necroinflammation score (0–18) (34) by an attending liver pathologist (S.K.) with 10 years of experience in a blinded fashion. In the case of discordant scores between the two lobes, the higher stage was used in the statistical analysis.

Morphometric Measurement of Hepatic Fibrosis

The extent of hepatic fibrosis was assessed morphometrically by a hepatologist (J.J.M.) who was blinded to the degree of rat CCl_4 exposure. The same picrosirius red-stained slices that were used to assign Ishak fibrosis scores (one tissue slice from the left hepatic lobe and one from the right) were analyzed for each liver. Each tissue slice was serially photographed 20 times at low-power magnification (original magnification, ×10) with preset XY stage movements to eliminate bias. For each tissue slice, fibrosis was measured as the mean percentage of total tissue area stained by picrosirius red per microscopic field (Simple PCI Software, Hamamatsu, Sewickley, Pa). White space was not included in area estimates. The results for the two tissue slices from each liver were then averaged to obtain the percentage of fibrosis area for each rat. This analysis was also conducted under blinded conditions by an attending hepatologist (J.J.M.) with 25 years of subspecialty experience.

Statistical Analysis

Uni- and multivariate linear regression was used to evaluate the relationship between the variables calculated at imaging, fECS and MMCM uptake, and the histopathologic reference standards, Ishak fibrosis score and morphometry. The R^2 value was used to assess the strength of this correlation, and P values less than .05 were considered to indicate a significant difference. Since all Ishak scores for necroinflammation were between 0 and 1, necroinflammation was excluded from analysis. The statistical analysis was performed (V.V., B.M.Y.) with computer software (Stata, version 8.0; Stata, College Station, Tex).

Figure 2

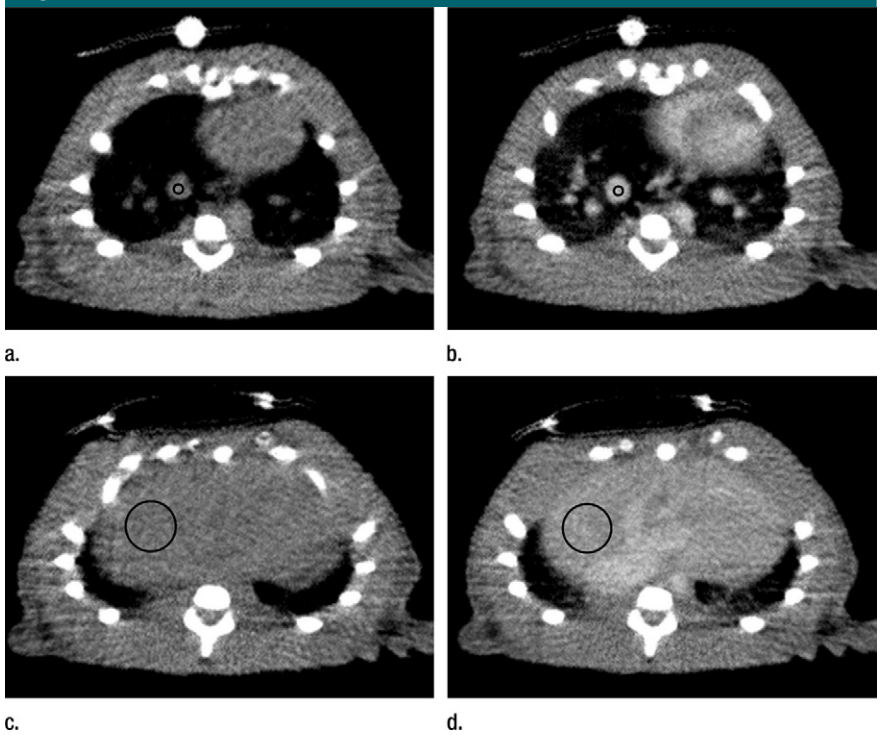

Figure 2: Micro-CT images and image processing. **(a)** Precontrast thoracic inferior vena cava and one of three ROIs used to measure blood pool attenuation. **(b)** Postcontrast inferior vena cava and corresponding ROI. **(c)** Precontrast liver and one of four ROIs used to measure hepatic attenuation. **(d)** Postcontrast liver and corresponding ROI.

Results

Carbon Tetrachloride Model

Ishak fibrosis scores ranged from 0 to 5 for the rats exposed to CCl_4, while Ishak scores for the control animals, which did not receive CCl_4, were all 0. The distribution of Ishak scores was as follows: Three rats had an Ishak score of 0; two rats, an Ishak score of 1; one rat, an Ishak score of 2; six rats, an Ishak score of 3; seven rats, an Ishak score of 4; and two rats, an Ishak score of 5. No rats had an Ishak score of 6. Nine of the treated animals had early stage hepatic fibrosis (Ishak fibrosis score of 0–3), and another nine had late-stage hepatic fibrosis (Ishak fibrosis score of 4 or 5) (Fig 3). None of the rats had frank cirrhosis, as designated by an Ishak score of 6. The distribution of necroinflammation scores was as follows: Nineteen rats had an Ishak score of 0, and two rats had an Ishak score of 1. Since no rats had necroinflammation scores of 2–18, necroinflammation was excluded from uni- and multivariate analyses. Morphometric analysis indicated that the amount of fibrosis in the rat livers ranged from 0.46% to 3.5% of the total liver area. One animal from the 10-week CCl_4 group was excluded from liver morphometry analysis due to inadequate histologic staining.

fECS Estimates

Twenty-one animals successfully underwent CT scanning with low-molecular-weight contrast materials. The calculated

Figure 3

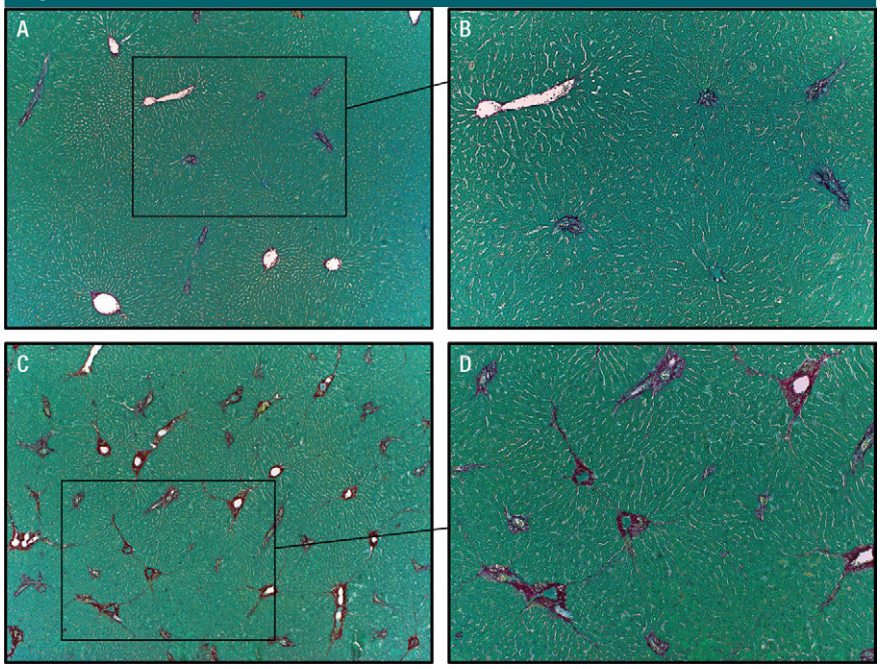

Figure 3: Photomicrographs of picrosirius red-stained liver slices. *A,* Slice obtained in a control animal with an Ishak fibrosis score of 0 (original magnification, ×5). *B,* Closer look at the same slice shown in *A* (original magnification, ×10). *C,* Slice obtained in an animal that received CCl_4 with an Ishak fibrosis score of 4 (original magnification, ×5). *D,* Closer look at the same slice shown in *C* (original magnification, ×10).

CT scan estimates of the fECS ranged from 11% to 37% (Fig 4). There was a strong correlation between fECS estimates and Ishak fibrosis scores (R^2 = 0.751, $P < .001$), as well as between fECS estimates and the liver fibrosis area (R^2 = 0.801, $P < .001$) (Fig 4, Table 1).

Macromolecule Uptake

Nineteen animals subsequently underwent successful CT with MMCM. MMCM was not successfully delivered to two rats due to poor tail vein access; one rat was in the 2-week CCl_4 group, and the other was in the 8-week group. A strong negative correlation was observed between the hepatic uptake of MMCM and the Ishak fibrosis score (R^2 = 0.827, $P < .001$), as well as between the hepatic uptake of MMCM and the liver fibrosis area (R^2 = 0.643, $P < .001$) (Fig 4, Table 1). Multivariate linear regression showed a trend toward independence for MMCM uptake and fECS in the prediction of Ishak fibrosis scores (adjusted R^2 value, 0.860; P = .081 and P = .033, respectively) (Table 2).

Discussion

Our results show that for early- and intermediate-stage liver fibrosis, CT measurements of both fECS and MMCM uptake individually correlate well with the degree of hepatic fibrosis, as measured with two histopathologic standards, the Ishak fibrosis score and morphometric measurements of fibrosis. Multivariate linear regression analysis also shows that there is a trend toward significance for these two contrast-enhanced CT estimates to be independent predictors of liver fibrosis.

Several noninvasive methods are currently under investigation for the quantification of liver fibrosis. These methods can be divided into two main categories: serum panels and imaging. Serum panels are useful when measuring the rate of hepatic fibrosis over time because they are readily performed on small samples of blood. While they are useful in excluding advanced fibrosis, they are unsuitable for staging because they cannot be used to reliably quantify the extent or regional distribution of hepatic fibrosis (7,8,35). The most widely successful imaging techniques focus on tissue strain imaging, known as elastography, and may be performed with either ultrasonography or magnetic resonance (MR) imaging. Like serum measurement, they are currently most reliable for distinguishing between early- and late-stage fibrosis (9,10). Dynamic contrast-enhanced CT and MR imaging, which focus on the initial phases of contrast material wash-in and washout, are technically challenging and require multiple repeat studies and do not appear as robust in the differentiation between early and late stages of liver injury (11,36). These CT and MR imaging techniques also typically require dedicated expertise (10,12,37).

The contrast-enhanced CT method we used to calculate fECS is complementary to these published methods in that it is used to study a distinctly different aspect of liver fibrosis than tissue strain or first-pass contrast kinetics. Instead, our low-molecular-weight contrast material method focuses on the equilibrium phase for fECS measurements and hence requires only two image sets: an unenhanced series and a delayed series. This method should be readily applicable to clinical scanning, with minimal disruption to current clinical protocols. However, the minimum scan delay for reliable estimation of the fECS is not well defined and is likely to be several minutes longer than is typical for current liver imaging protocols, particularly when a large amount of fibrosis is present. Prior studies of fibrous scars and fibrotic tumors of the liver, such as cholangiocarcinomas, suggest that scan delays of at least 10–15 minutes are needed for optimal visualization of related fibrosis (38,39). While our preliminary results are promising, further work is needed to validate the value of equilibrium phase imaging in the evaluation of liver fibrosis in different scenarios, such as active liver inflammation or elevated hepatic venous pressures from right-sided heart failure, which may

also result in expansion of the extracellular space. In our CCl_4 liver fibrosis model, substantial liver inflammation was not present. Notably, such confounders also affect both serologic and stiffness tests of hepatic fibrosis.

We hypothesize that the strong inverse correlation we observed between MMCM uptake and hepatic fibrosis severity relates to the known reduction in the permeability of liver sinusoidal endothelial cells to macromolecules in the setting of hepatic fibrosis. The PEG12000-Gen 4-IOB contrast material was designed to be biocompatible, potentially clinically feasible, and similar in size to albumin. Previous invasive studies have shown that the uptake of labeled albumin in a surgical in situ liver perfusion model dramatically decreases in cirrhotic livers due to the loss of functional sinusoidal endothelial fenestrations (25). A prior MR imaging study on rabbits also showed a reduced distribution volume of macromolecules in fibrotic livers (26). Our MMCM results build on this prior work by demonstrating a strong correlation between a simplified noninvasive CT scanning measure and hepatic fibrosis. Further work will be needed to optimize the measurements of MMCM uptake. In particular, a study is needed to address the question of whether simple delayed imaging scans or repeated dynamic contrast-enhanced imaging with kinetic fitting to two-compartment models are best for obtaining robust results (29).

There were several limitations to our study. First, micro-CT rather than clinical CT was used for the scans. While this provided slightly greater spatial resolution than that available with a clinical CT scanner and enabled the use of respiratory gating, the acquisition time was much longer than that with a clinical scanner and thus predisposed the images to whole-body motion artifacts. Second, frank cirrhosis, which is characterized as an Ishak fibrosis score of 6, was not induced in our animal cohort. We focused on the early and intermediate stages of fibrosis, and future work will be needed to validate these results in the setting of

Figure 4

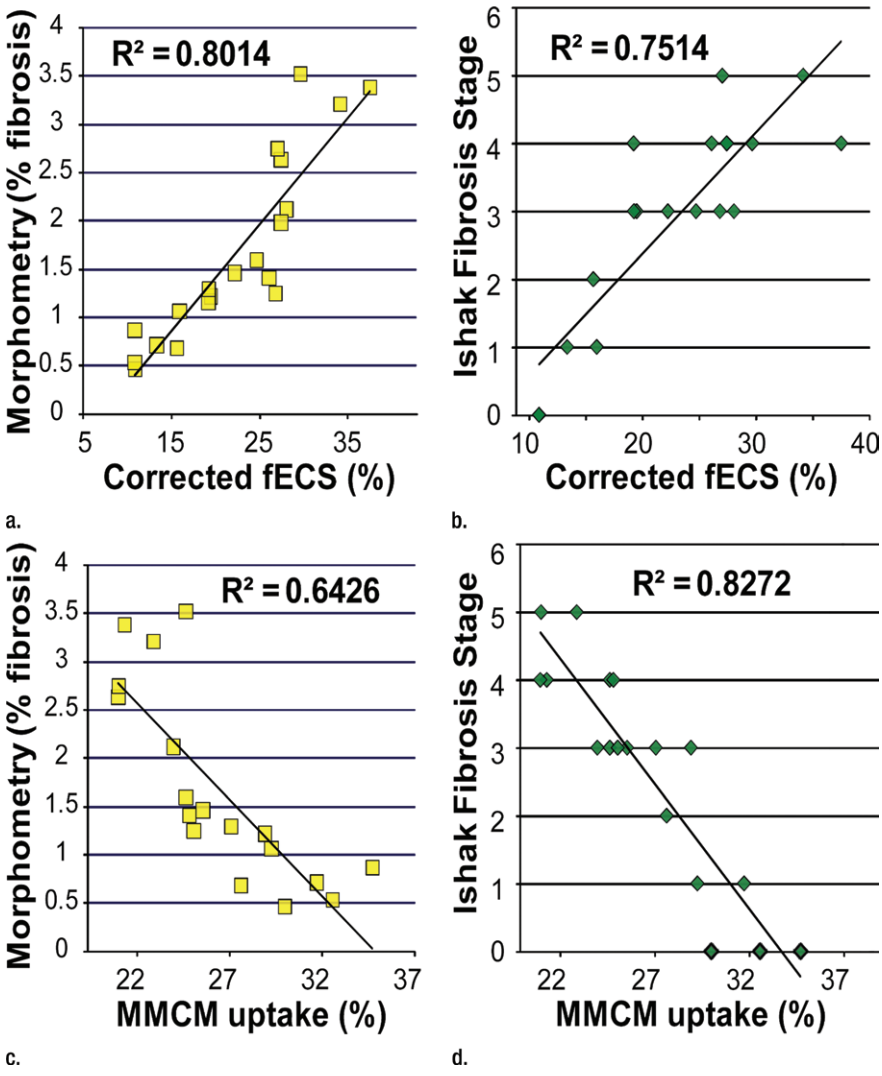

Figure 4: Scatterplots of calculated fECS and MMCM uptake values against two histopathologic standards, Ishak fibrosis scores and morphometric measurements of percent fibrosis area. Lines in each plot represent regression lines used to predict the reference standard outcomes from the relevant CT measures. **(a)** Corrected fECS versus percent fibrosis area. **(b)** Corrected fECS versus Ishak fibrosis scores. **(c)** MMCM uptake versus percent fibrosis area. **(d)** MMCM uptake versus Ishak fibrosis scores.

Table 1

Univariate Linear Regression Analysis Comparing CT Quantification of fECS and MMCM Uptake with Histopathologic Measures of Hepatic Fibrosis

	Percent Fibrosis Area		Ishak Score	
Variable	R^2 Value	*P* Value	R^2 Value	*P* Value
fECS	0.801	<.001	0.751	<.001
MMCM uptake	0.643	<.001	0.827	<.001

Table 2

Multivariate Linear Regression Analysis Comparing CT Quantification of fECS and MMCM Uptake to Histopathologic Measures of Hepatic Fibrosis

	Percent Fibrosis Area		Ishak Score	
Variable	R^2 Value	*P* Value	R^2 Value	*P* Value
fECS	0.803	.003	0.860	.081
MMCM uptake	…	.875	…	.033

more severe hepatic fibrosis. Nevertheless, the accurate quantification of early- and intermediate-stage liver fibrosis is of greatest clinical need since these early stages are most amenable to fibrolytic therapy. Third, although two separate histopathologic reference standards were studied, an ideal reference standard does not exist. Histopathology is prone to sampling error, technical variation, and, as in the case of Ishak scoring, subjectivity. Fourth, to our knowledge, a CT MMCM is not yet clinically available, although several are under preclinical study.

In summary, contrast-enhanced CT measurements of fECS and MMCM uptake may be useful semiquantitative markers of liver fibrosis and could enable noninvasive monitoring of liver disease severity.

Disclosures of Conflicts of Interest: V.V. No relevant conflicts of interest to disclose. **Y.F.** No relevant conflicts of interest to disclose. **J.J.M.** No relevant conflicts of interest to disclose. **D.G.** No relevant conflicts of interest to disclose. **S.K.** No relevant conflicts of interest to disclose. **M.C.C.** No relevant conflicts of interest to disclose. **B.M.Y.** Financial activities related to the present article: none to disclose. Financial activities not related to the present article: is a consultant to GE Healthcare and Siemens Medical Systems; institution has grants pending with GE Healthcare and Medrad; gave lectures for GE Healthcare. Other relationships: none to disclose.

References

1. Goldin RD, Goldin JG, Burt AD, et al. Intra-observer and inter-observer variation in the histopathological assessment of chronic viral hepatitis. J Hepatol 1996;25(5):649–654.
2. Bedossa P, Poynard T, Naveau S, Martin ED, Agostini H, Chaput JC. Observer variation in assessment of liver biopsies of alcoholic patients. Alcohol Clin Exp Res 1988;12(1):173–178.
3. Poniachik J, Bernstein DE, Reddy KR, et al. The role of laparoscopy in the diagnosis of cirrhosis. Gastrointest Endosc 1996;43(6):568–571.
4. Maharaj B, Maharaj RJ, Leary WP, et al. Sampling variability and its influence on the diagnostic yield of percutaneous needle biopsy of the liver. Lancet 1986;1(8480):523–525.
5. Pagliaro L, Rinaldi F, Craxì A, et al. Percutaneous blind biopsy versus laparoscopy with guided biopsy in diagnosis of cirrhosis: a prospective, randomized trial. Dig Dis Sci 1983;28(1):39–43.
6. Seeff LB, Everson GT, Morgan TR, et al. Complication rate of percutaneous liver biopsies among persons with advanced chronic liver disease in the HALT-C trial. Clin Gastroenterol Hepatol 2010;8(10):877–883.
7. Parkes J, Guha IN, Roderick P, Rosenberg W. Performance of serum marker panels for liver fibrosis in chronic hepatitis C. J Hepatol 2006;44(3):462–474.
8. Grigorescu M. Noninvasive biochemical markers of liver fibrosis. J Gastrointestin Liver Dis 2006;15(2):149–159.
9. Friedrich-Rust M, Ong MF, Herrmann E, et al. Real-time elastography for noninvasive assessment of liver fibrosis in chronic viral hepatitis. AJR Am J Roentgenol 2007;188(3):758–764.
10. Hotta N, Ayada M, Okumura A, et al. Noninvasive assessment of liver disease: measurement of hepatic fibrosis using tissue strain imaging. Clin Imaging 2007;31(2):87–92.
11. Rouvière O, Yin M, Dresner MA, et al. MR elastography of the liver: preliminary results. Radiology 2006;240(2):440–448.
12. Stebbing J, Farouk L, Panos G, et al. A meta-analysis of transient elastography for the detection of hepatic fibrosis. J Clin Gastroenterol 2010;44(3):214–219.
13. Dienstag JL, Goldin RD, Heathcote EJ, et al. Histological outcome during long-term lamivudine therapy. Gastroenterology 2003;124(1):105–117.
14. Falize L, Guillygomarc'h A, Perrin M, et al. Reversibility of hepatic fibrosis in treated genetic hemochromatosis: a study of 36 cases. Hepatology 2006;44(2):472–477.
15. Mallet V, Gilgenkrantz H, Serpaggi J, et al. Brief communication: the relationship of regression of cirrhosis to outcome in chronic hepatitis C. Ann Intern Med 2008;149(6):399–403.
16. Veldt BJ, Heathcote EJ, Wedemeyer H, et al. Sustained virologic response and clinical outcomes in patients with chronic hepatitis C and advanced fibrosis. Ann Intern Med 2007;147(10):677–684.
17. Friedman SL. Molecular regulation of hepatic fibrosis, an integrated cellular response to tissue injury. J Biol Chem 2000;275(4):2247–2250.
18. Friedman SL. Mechanisms of hepatic fibrogenesis. Gastroenterology 2008;134(6):1655–1669.
19. Jacobson IM, McHutchison JG, Dusheiko G, et al. Telaprevir for previously untreated chronic hepatitis C virus infection. N Engl J Med 2011;364(25):2405–2416.
20. Dixon JB, Bhathal PS, Hughes NR, O'Brien PE. Nonalcoholic fatty liver disease: improvement in liver histological analysis with weight loss. Hepatology 2004;39(6):1647–1654.
21. Fowell AJ, Iredale JP. Emerging therapies for liver fibrosis. Dig Dis 2006;24(1-2):174–183.
22. Villeneuve JP, Dagenais M, Huet PM, Roy A, Lapointe R, Marleau D. The hepatic microcirculation in the isolated perfused human liver. Hepatology 1996;23(1):24–31.
23. Afdhal NH, Nunes D. Evaluation of liver fibrosis: a concise review. Am J Gastroenterol 2004;99(6):1160–1174.
24. Sahin S, Rowland M. Estimation of aqueous distributional spaces in the dual perfused rat liver. J Physiol 2000;528(Pt 1):199–207.
25. Reichen J. The role of the sinusoidal endothelium in liver function. News Physiol Sci 1999;14:117–121.
26. Van Beers BE, Materne R, Annet L, et al. Capillarization of the sinusoids in liver fibrosis: noninvasive assessment with contrast-enhanced MRI in the rabbit. Magn Reson Med 2003;49(4):692–699.
27. Reichen J, Egger B, Ohara N, Zeltner TB, Zysset T, Zimmermann A. Determinants of hepatic function in liver cirrhosis in the rat: multivariate analysis. J Clin Invest 1988;82(6):2069–2076.
28. Whitehouse G, Worthington B. Techniques in diagnostic imaging. 3rd ed. Cambridge, Mass: Blackwell Science, 1996.

29. Shames DM, Kuwatsuru R, Vexler V, Mühler A, Brasch RC. Measurement of capillary permeability to macromolecules by dynamic magnetic resonance imaging: a quantitative noninvasive technique. Magn Reson Med 1993;29(5):616–622.

30. Raatschen HJ, Fu Y, Brasch RC, Pietsch H, Shames DM, Yeh BM. In vivo monitoring of angiogenesis inhibitory treatment effects by dynamic contrast-enhanced computed tomography in a xenograft tumor model. Invest Radiol 2009;44(5):265–270.

31. McLean EK, McLean AE, Sutton PM. Instant cirrhosis: an improved method for producing cirrhosis of the liver in rats by simultaneous administration of carbon tetrachloride and phenobarbitone. Br J Exp Pathol 1969;50(5):502–506.

32. Proctor E, Chatamra K. High yield micronodular cirrhosis in the rat. Gastroenterology 1982;83(6):1183–1190.

33. Fu Y, Nitecki DE, Maltby D, et al. Dendritic iodinated contrast agents with PEG-cores for CT imaging: synthesis and preliminary characterization. Bioconjug Chem 2006;17(4):1043–1056.

34. Ishak K, Baptista A, Bianchi L, et al. Histological grading and staging of chronic hepatitis. J Hepatol 1995;22(6):696–699.

35. Poynard T, McHutchison J, Manns M, Myers RP, Albrecht J. Biochemical surrogate markers of liver fibrosis and activity in a randomized trial of peginterferon alfa-2b and ribavirin. Hepatology 2003;38(2):481–492.

36. Kim T, Murakami T, Takahashi S, Hori M, Tsuda K, Nakamura H. Diffusion-weighted single-shot echoplanar MR imaging for liver disease. AJR Am J Roentgenol 1999;173(2):393–398.

37. Aguirre DA, Behling CA, Alpert E, Hassanein TI, Sirlin CB. Liver fibrosis: noninvasive diagnosis with double contrast material-enhanced MR imaging. Radiology 2006;239(2):425–437.

38. Asayama Y, Yoshimitsu K, Irie H, et al. Delayed-phase dynamic CT enhancement as a prognostic factor for mass-forming intrahepatic cholangiocarcinoma. Radiology 2006; 238(1):150–155.

39. Brancatelli G, Baron RL, Federle MP, Sparacia G, Pealer K. Focal confluent fibrosis in cirrhotic liver: natural history studied with serial CT. AJR Am J Roentgenol 2009;192(5):1341–1347.